Published by :
http://www.ijert.org

International Journal of Engineering Research & Technology (IJERT)
ISSN: 2278-0181
Vol. 10 Issue 02, February-2021

Experimental and Theoretical Study of the Heavy Vehicle Dynamics Loads on Terrain

M M M Salem
Automotive and tractor Eng. Dept
Faculty of Engineering, Minia University
Minia, Egypt

K.A. Abd El-Gawwad
Automotive and tractor Eng. Dept
Faculty of Engineering, Minia University
Minia, Egypt

Abstract - It is well known that there is a strong connection between wheel loads of heavy moving vehicles and the behavior of the soil. This relationship can be entirely determined if the stress in the soil for heavy car loads and soil conditions are correctly defined. A mathematical model to predict the heavy load (dynamic and static) of the wheel on soils was implemented in this paper. In addition, under the floor surface, the vertical, the radial and tangential stresses showed different values of soil depth and different soil types. The insufficiency load was described by experimental laboratory experiments using five soil types. The required soil, which could be used without fail for the heavy vehicle motion, could be chosen from experimental and theoretical results.

Keywords,- Heavy vehicle, dynamic wheel load, random input, soil stresses and soil properties.

I. INTRODUCTION

A large number of off-road equipment moves over the terrain. In view of the number of tractors and agricultural soil growing equipment used, the number of earthmoving machines used in the construction industry, the number of off-road lorries used in the off-road transportation industry and the number of military vehicles used for combat and logistic purposes. One of these devices can understand the degree to which terramechanics are applicable, as they are concerned with soil stress below ground surface as a result of the movement of off-road devices.

The loading of the wheels (dynamic load exerted by a tyre, the weight distribution static load) is critical to the performance of the heavy vehicle. There is also evidence that this load influences ground tension under the pneumatic. One cause of the pressure on the building and the downward collapse of the building is the stress distribution below the land area because of both the impact of wheel loads on the earth and the transported load effect at different depths of the soil. The accurate prediction of this soil stress is a complex issue, taking into account the dynamic wheel load, the various soil types, various soil layers and soil water.

A large number of studies concern with the study of stress distribution at contact area between tyre and soil [1-5]. N. Nankali et al [6] studied the effect of dynamic load on soil Stress Analysis of Tractor Tire Interacting with Soil using 2D Finite Element Method. Hao Li and Christian Schindler **[7]** presented the Analysis of soil compaction and tire mobility with finite element method Also, Road Vehicle Suspension Design, Dynamics, and Control **by** Dongpu Cao et al [8]. M. Agostinacchio et al [9] presented The vibrations induced by surface irregularities in road pavements**.** In the light of the previous available researches in this field, it can be say that very little information is available on soil stresses distribution below terrain surface. So, the main objectives of this research towards to:

1-To develop a mathematical model for the heavy vehicle and the terrain properties. This model used to predict the heavy vehicle wheel loads (dynamic and static) affect terrain surface.

2-To estimate the soil stresses (vertical, radial and tangential) resulted from the effect of wheel load over different types of soil and at different soil depth.

3-To carry out laboratory tests to measure the failure load of selected five types of soil and to evaluate the stresses in soil under the measured failure load.

4-To select the best suitable soil, with which the heavy vehicle can be moved without soil failure.

II. THE HEAVY VEHICLE DYNAMIC MODEL

The Fig. 1 shows an 8-degree schematic diagram. The model for two-axled heavy-duty vehicle ridings consists of three masses connected by linear spring and damper elements that create dynamic forces based on their relative positions and speeds. Also, the tyres, Sharp, R.S. and Crolla, D. A., [10], were modeled as linear vertical spring and damper. The model has 8 degrees of freedom based on the second law of Newton's motion. It is represented by the steady state of a vehicle in order that, because of the static deflection of the suspension components, the effect of mass gravity conditions can be lost with forces. The eight-degrees of freedom in the model are representing to the bounce movements of the driver seat X_{ds}, the four road wheels $X_{wi}, i = 1$ to 4 and the body X_h, beside the pitch and roll movements θ_p and θ_r of the body. The model contains two categories of the dynamic forces. First, the suspension forces of the driver seat and four road wheels are representing by $F_{ds}, F_{sw1}, F_{sw2}, F_{sw3}$ and F_{sw4}. Second, the dynamic road wheels loads are representing by F_{rw1}, F_{rw2}, F_{rw3} and F_{rw4}. The parameters of the eight degrees of freedom model are taken as shown in the selected heavy vehicle catalogue. The equations of motion are written as:

$$\ddot{X}_{ds} = F_{ds} / M_{ds} \quad (1)$$

International Journal of Engineering Research & Technology (IJERT)
ISSN: 2278-0181
Vol. 10 Issue 02, February-2021

$$\ddot{X}_{w1} = (F_{rw1} - F_{sw1})/M_{w1} \quad (2)$$

$$\ddot{X}_{w2} = (F_{rw2} - F_{sw2})/M_{w2} \quad (3)$$

$$\ddot{X}_{w3} = (F_{rw3} - F_{sw3})/M_{w3} \quad (4)$$

$$\ddot{X}_{w4} = (F_{rw4} - F_{sw4})/M_{w4} \quad (5)$$

$$\ddot{X}_{h} = \left(\sum_{i=1}^{4} F_{swi} - F_{ds}\right)/M_{h} \quad (6)$$

$$\ddot{\theta}_{p} = \left(\sum_{i=3}^{4} F_{swi}\cdot a_r + F_{ds}\cdot a_{ds} - \sum_{i=1}^{2} F_{swi}\cdot a_f\right)/I_p \quad (7)$$

$$\ddot{\theta}_{r} = \left[b.\left((F_{sw1} + F_{sw2}) - (F_{sw3} + F_{sw4})\right) + b_{ds}.F_{ds}\right]/I_r \quad (8)$$

Inputs to the model take the form of wheel displacements generated by the vehicle traversing over a ground profile. These inputs are independent so that, a rear wheel input is simply a delayed version of a front wheel input, and near side inputs may be correlated by an amount dependent on their distance apart. An artificial road input time history $X_0(t)$ of the road profile can be generated from the spectral density function $PSD(f)$ of a given road by using digital processing involving the inverse discrete Fourier transform, Ruf [11], Robson [12] and Cebon and Newland [13]. The road $PSD(f)$ formula of the collared noise function is

$$PSD(f) = C \cdot V^{1.5} \cdot f^{-2.5} \quad (9)$$

Where f is the frequency (up to 15 Hz), C is the road roughness constant and V is the forward vehicle speed.

The heavy vehicle model moving over terrain soil is solved as a non-linear because the soil deformation sinkage $Z_k(t)$ created during the heavy vehicle movements over the terrain profile. The soil deformation sinkage produced under wheels calculated here by equation (10). The generation of the artificial road input time history $X_0(t)$ of the road profile could be used directly as input to the front wheels. The rear wheels running behind the front by a lag time l_t. Subtracting the total soil deformation sinkage from the road profile, will modify the rear wheels input as the following equation:

$$X_{or}(t) = X_o(t + l_{tr}) - Z_k(t), \quad (10)$$

III. STRESS DISTRIBUTION IN SOIL

A large proportion of soil engineering problems require an understanding of the soil stress behaviour. Also, the analysis of the relationships between applied load and contact area, soil depth and settlement due to applied load is one of the key problems of the land relative to applied loads. In fact, these relationships are very complex with regard to the soil characteristics and to different load values. In this area, the theoretical studies have included a number of hypotheses to simplify the understanding of this phenomenon. The stress below the surface of the ground is due to the soil's self-weight and load. The effect of heavy car wheel load on the soil stresses is investigated in this paper. The overall static load of the wheel is expected to be the results of the distribution of weight and the maximum dynamic load on the wheel. The Boussinesq theory of Stress helps with this assumption. The theoretical results of elastic theory in the most basic case of loading acts on a solid, homogenous, elastic, semi-infinite, and weightless medium are used to support this theory. The charge is vertical, pointing, on the horizontal boundary surface In this case (road surface). Radial distribution of stresses in the semi-infinite medium is assumed in one and only concentrated load. The assumptions of Boussinesq are that the earth is weightless, the soil is stress-free before the effect of pointing, stress continuity, and stress symmetrical axis. The pointed load of the semi-infinite mass surface is shown in Figure 2. The following equal parameters include the vertical stress on a horizontal plane, radial stress and tangential stress[14].

$$\sigma_z = 3Pz^3/2\pi R^5 \quad (11)$$

$$\sigma_r = -P\left[\left(-3r^2 z/R^3\right) + (1-2\upsilon)R/(R+z)\right]/2\pi R^2 \quad (12)$$

$$\sigma_\theta = -(1-2\upsilon)P\left[(z/R) - R/(R+z)\right]/2\pi R^2 \quad (13)$$

The above equations shows that the vertical stress depends on the ratio of Poisson, while the radial and tangential stresses depend on the ratio of Poisson.

IV. TESTING MOULD AND LOADING SYSTEM

The model consists of a 30 cm long, 30 cm wide, and 30 cm high stainless steel box. Mold material's wall thickness is 10 mm. Static loading with a rigid footing was the loading method used in this analysis. This foundation had a width of 5.7cm and a length of 7.1cm. It reflects the wheel truck dimensions of the selected magnitude. The base was fixed to a steel rod of 5 cm in diameter and 20 cm in height and soldered at the top of the rod to a circular plate of 10 cm diameter and 2.5 cm thick. This method ensures that the load over the footprint of 5.7 to 7.1cm is spread. The charge was measured with a 300kN compression machine with a precision of 0,1kN. Fig.3 displays a complete configuration of the model.

V. MATERIALS USED

A number of bearing capacity tests were performed in laboratory on five types of soil to analyze the load applied, contact area, soil depth and settlement of soil due to the applied load. In the present experiments five types of materials have been used. Silty clay, coarse sand, stoned lime, sandy gravel and gravel sand are the forms. These soils are used on the unpaved road as base layer. Tests were performed to determine the physical characteristics of these soil types. Figure 4 shows the grain distribution curves and Table 1 shows the physical properties measured for the various soils used for the experiments.

Table (1): Physical properties of used soil

ROPERTY	Silty clay	Coarse sand	Gravely sand soil (Hepa)	Lime stone	Sandy gravel soil
G_s	2.71	2.56	2.61	2.52	2.83
L.L.	62.5	NL	27	NL	28
P.L.	23.1	NP	16	NP	6
$\gamma_{d\,max}$ gm /cm^3	1.63	1.854	2.18	1.925	2.25
OMC%	17.9	7.85	8	6	7.5
C_u kN/m^2	70	0	0	0	0
ϕ_u	11°	35.7°	41.3°	40.2°	45.7°

International Journal of Engineering Research & Technology (IJERT)
ISSN: 2278-0181
Vol. 10 Issue 02, February-2021

VI. EXPERIMENTAL PROGRAM AND PROCEDURES

In the experimental program of this study, we measured the load of failures (ultimate load) that can be performed in the base course samples. All of the experiments have been conducted using an automating compactor to compress the base layers in the model with optimum dry density γd_{max} and optimal moisture content (O.M.C). The modified proctor compaction tests were carried out at the laboratory to determine the values of (O.M.C.) for each sample. Each layer equal to 5cm, the soil is compacted in the model. Compact soil finished at 20cm thick. A compression-testing computer was used to statically load. At a constant load rate of 0,5 kN/min, all tests were completed. The deformities were measured with a 25mm dial gage and 0.01 mm accuracy and were also automatically measured with the measuring system.

VII. RESULTS AND ANALYSIS

To solve these models, there are three computer programs using MATLAB software. The first software is designed to get time-domain road input and figure. 5 displays the soil input spontaneously in the history of the front wheels. While the road under the rear wheels shifts like equations (10). The parameters for the road formula are 15 Hz frequency and $5*10^6$ road rugging. The second software is designed to obtain variable randomly dynamic loads of wheels, and an example is given in the Figure 6 for the proportion of the dynamic force for wheels for front wheels.

The third program consists of the equations explained in the stress-shifting portion of the soil under the terrain surface. The results of different tests are shown in Fig. 7, which gives the relation between the applied load and the settlement associated. As shown from Fig. 7, the sandy gravel soil gave the higher value of load with settlement compared with the other types of soils. Also, from the figure it can be seen that the value of applied load was increased with settlement without peak value for sandy gravel soil, limestone soil and silty clay soil. For case of using gravely sand soil, and coarse sand soil, the load peak value was obtained as shown in the figure. As a conservation of the two direct portions of the applied load-settlement curve (Feee load) was taken as the intersection as illustrated in Fig. 8, or in case of the full load, the maximum load value. Figure 9 shows the failure load values for the various types of soil used. Lime, sandy gravel, raw sand, Hepa and stubborn clay (56, 75, 8, 13.5 and 4.5) have tons failing at kN. Based on the findings in Fig. 9, it can be said that, sandy gravel soil is the highest, then calcareous gravel, and gross sand, and silty clay soils are the worst soil.

With a static and dynamic impact of wheel load, heavy vehicle movement projected stress on the ground and shown in Figures 10 to 13.. Figure 10 (a, b, c) shows the distribution by horizontal distance from the vertical axis of the tyre, of the vertical, radial, tangent stresses at various Poisson values of the ratio. The ratio of Poisson ranged from 0.2 to 0.5 m at ground depth, and 15 kN was caused by the movement of heavy vehicles over sand soil. The vertical stresses do not differ from the pneumatic vertical axis in the horizontal span, whereas radial and tangential stresses in the soil vary. The radial stress has increased by increasing the Poisson ratio, while the tangent stress is increased to around 0.63 m and decreased afterwards by increasing the Poisson ratio. The radial stress has increased. The distribution of stresses in the soil with the adjustment of the ratio of Poißon along the depth of the soil at a horizontal distance of 0.3 m is shown in Fig. 11 (a, b and c). The horizontal distance effect on soil stresses can be seen in Fig. 12 (a, b, and c). At Poisson, the horizontal distance ranged from 0,2m to 0,6m and sand. The vertical stress is decreased while the radial stress increases as the horizontal gap is increased. The direction of the highest stress peak is also modified with different amounts of horizontal distance. Fig.13 (a, b and c) presents a horizontal distance to distance from the vertical tyre axis for distribution of stress on soil at varying values of soil depth. At the Poisson ratio of 0.3, soil depth ranged from 0.6 m to 1.2 m and stress on the sand surface. The figure shows that the vertical stress and radial stress decrease, as the soil depth increases, while the tangential stress increases with the soil depth and decreases after a horizontal distance of about 0.63 m.

The results of experimental work compared the wheel load value of 15 kN to the soil of the heavy vehicle obtained from theoretical work were achieved. The results were calculated. It can be seen that the heavy vehicle used can be driven across sandy gravel and calcareous soils without any soil loss. While the soil will fail with the hefty vehicle movement in the case of coarse sand, hepa and silty clay. It is safe to assume, therefore, that sandy gravel soil is the best soil.

VIII. Conclusions

1. The model developed gives the historical wheel load effect to soil stresses.
2. The ratio of Poisson affects the radial and tangential stresses clearly.
3. As soil depth and the horizontal distance from a vertical tire axis increases, the vertical stress decreases.
4. On the basis of theoretical and test performance, the heavy vehicle used can be driven over the following soil types without soil insufficiency: sandy gravel soil accompanied by lime stone. It is safe to assume, therefore, that sandy gravel soil is the best type of soil.

References

[1] Shoya Higaa, Kazumasa Sawadaa, Kenji Nagaokaa, Keiji Nagatanib, and Kazuya Yoshidaa "Three-Dimensional Stress Distribution on a Rigid Wheel Surface for A LightWeight Vehicle" Proceedings of the 13th ISTVS European Conference, Rome, October 21–23, 2015.

[2] Omar González Cueto , Ciro E. Iglesias Coronel, Carlos A. Recarey Morfa, Guillermo

International Journal of Engineering Research & Technology (IJERT)
ISSN: 2278-0181
Vol. 10 Issue 02, February-2021

"Three dimensional finite element model of soil compaction caused by agricultural tire traffic" Elsevier, Agriculture 99 (2013) 146–152.

[3] Ainalem Nega and Hamid Nikraz "Evaluation of Tire-Pavement Contact Stress Distribution of Pavement Response and Some Effects on the Flexible Pavements" Airfield and Highway Pavements , DOI: 10.1061/9780784480946.016, 2017.

[4] Hao Li and Christian Schindler "Three-dimensional finite element and analytical modelling of tyre–soil interaction" Proc IMechE Part K: J Multi-body Dynamics 227(1) 42–60, 2012.

[5] J Pytka "Determining and analysing the stress state under wheeled-vehicle loads" Proc. IMechE Vol. 223 Part D: J. Automobile Engineering, 2009

[6] N. Nankali, M. Namjoo and M. R. Maleki "Stress Analysis of Tractor Tire Interacting with Soil using 2D Finite Element Method" Int J Advanced Design and Manufacturing Technology, Vol. 5/ No. 3/ June – 2012.

[7] Hao Li and Christian Schindler "Analysis of soil compaction and tire mobility with finite element method" Proc IMechE Part K: J Multi-body Dynamics 227(3) 275–291 ,IMechE 2013.

[8] Dongpu Cao, Xubin Song and Mehdi Ahmadian "Road Vehicle Suspension Design, Dynamics, and Control" Special Issue on "Advanced Suspension Systems and Dynamics for Future Road Vehicles" Journal of Vehicle System Dynamics, 2010

[9] M. Agostinacchio, D. Ciampa and S. Olita "The vibrations induced by surface irregularities in road pavements – a Matlab® approach" Eur. Transp. Res. Rev. (2014) 6:267–275, DOI 10.1007/s12544-013-0127-8.

[10] Sharp, R.S. and Crolla, D. A., "Road vehicle suspension design – a review", Vehicle System Dynamics, 16, pp. 167-192, 1987.

[11] Ruf, G., "The calculation of the vibration of a four-wheeled vehicle. Induced by random road roughness of the left and right track", Vehicle System Dynamics, 7, pp. 1-23, 1978.

[12] Robson, J.D., "Road surface description and vehicle response", Int. J. of vehicle design, 1, pp. 25-35, 1979.

[13] Cebon, D. and Newland, D.E., "The artificial generation of road surface topography by the inverse FFT method", Proc. 8th IAVSD Symp. On Dynamic of Vehicles on Roads and on Railway Tracks (Ed.J.K. Hedrick), Cambridge MA, pp. 1-12, 1983.

[14] Jumikis, A. R., "Soil Mechanics", D. Van Nortrand Company, Inc.,

NOMENCLATURE

a_{ds} & b_{ds} : The distances between the body center of gravity and the driver seat, m.

a_f & a_r : The distances between the body center of gravity and the front and rear wheels, m.

b : Wheel Track, m.

F_{ds} , : The suspension force of the driver seat, kN.

F_{rw} : Dynamic wheel load, kN.

F_{sw} : Suspension force, kN

International Journal of Engineering Research & Technology (IJERT)
ISSN: 2278-0181
Vol. 10 Issue 02, February-2021

I_p : The body pitch moment of inertia, kg.m^2.

M_{ds} : Mass of the driver seat, kg.

M_w : Wheel mass, kg.

M_h : Body mass, kg.

P : Vertical point load, kg.

X_0 & X_{or} : The randomly imposed displacement of the front and rear wheels, m.

X_w : The vertical randomly displacement of the wheels, m.

Z : Depth of soil, m.

ν : Poisson's ratio.

σ_z : Vertical stress, kN/m^2.

σ_r : Radial stress, kN/m^2.

σ_θ : Tangential stress, kN/m^2.

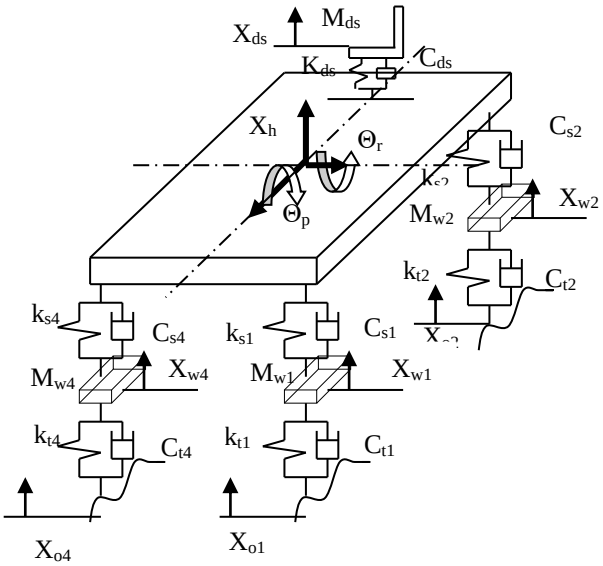

Fig. 1 A schematic diagram of 8 degrees of freedom

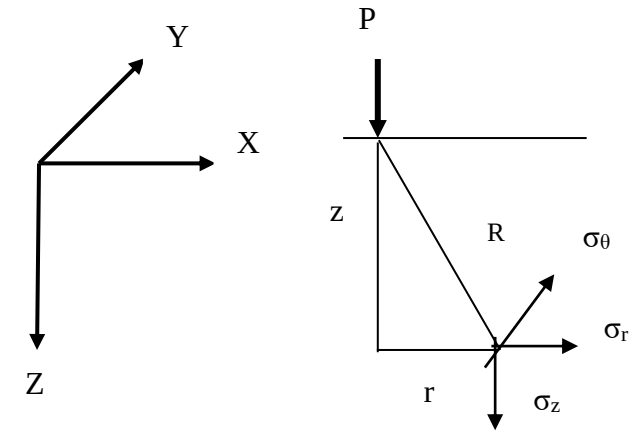

Fig. 2: Stresses due to a vertical pointed load on the surface of a semi-infinite layer.

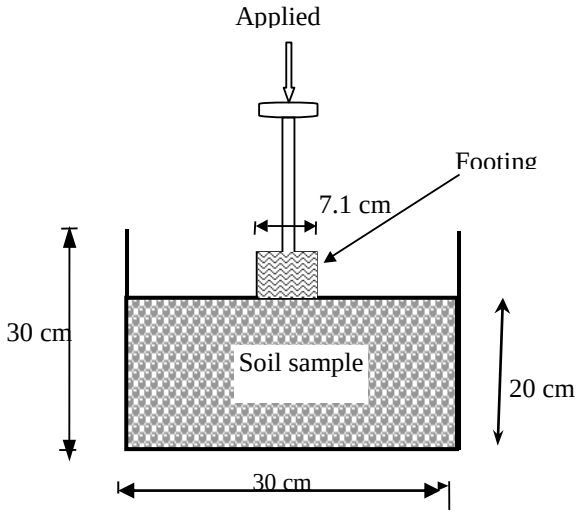

Fig.3: Testing set-up

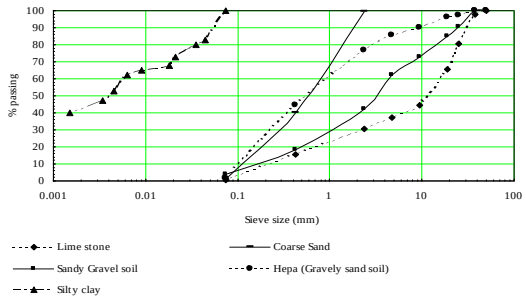

Fig.4: Grain size distribution of used soil

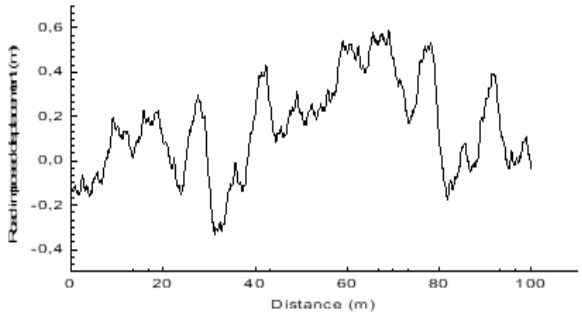

Fig. 5: The road input.

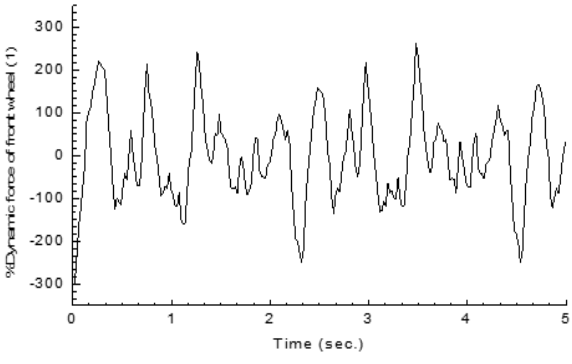

Fig. 6: The percentage dynamic wheel load on wheel No. (1)

International Journal of Engineering Research & Technology (IJERT)
ISSN: 2278-0181
Vol. 10 Issue 02, February-2021

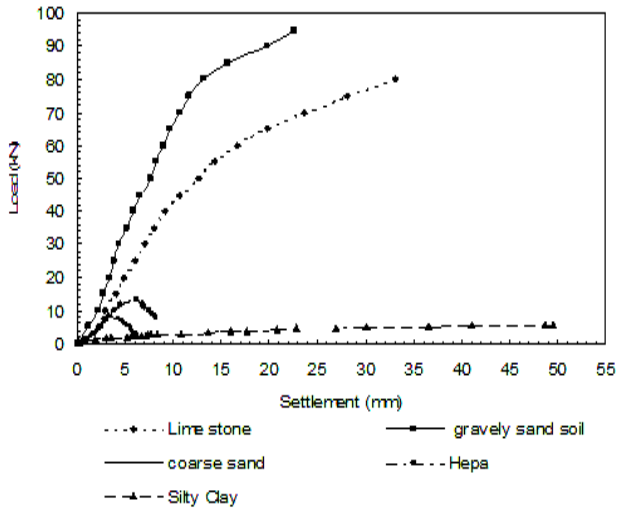

Fig. 7: Determination of ultimate load capacity (Failure load)

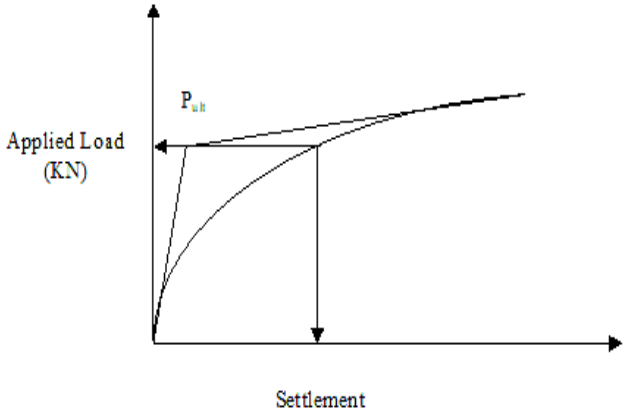

Fig. 8: Determination of ultimate load capacity (Failure load).

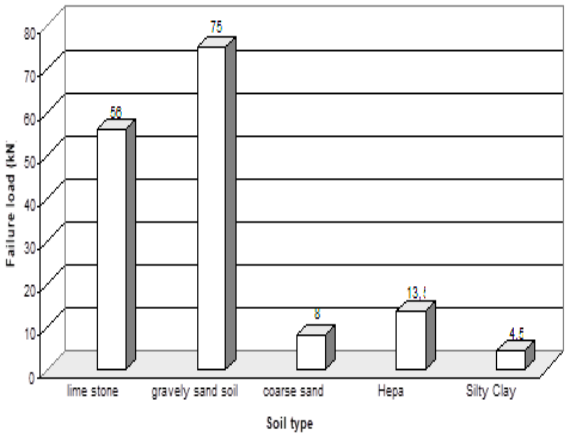

Fig.9: Values of failure load for different soil

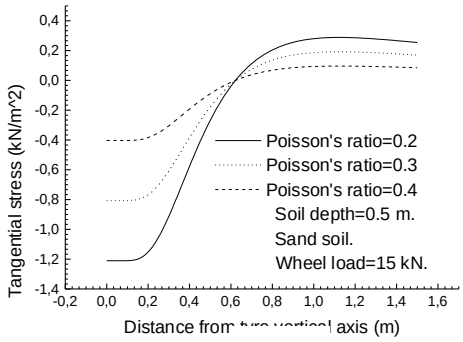

(a)

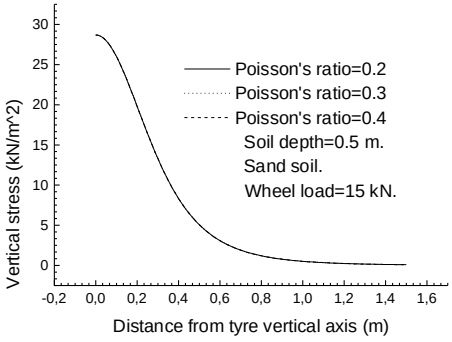

(b)

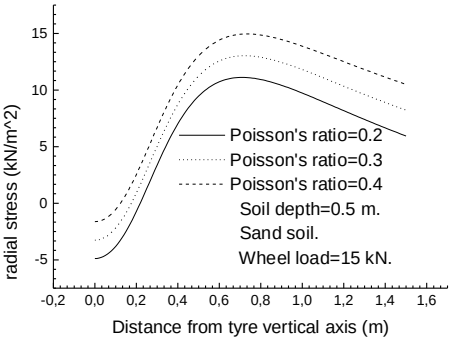

(c)

Fig. 10 Vertical, radial and tangential soil stresses distribution along the horizontal distance with the variation of Possion's ratio.

International Journal of Engineering Research & Technology (IJERT)
ISSN: 2278-0181
Vol. 10 Issue 02, February-2021

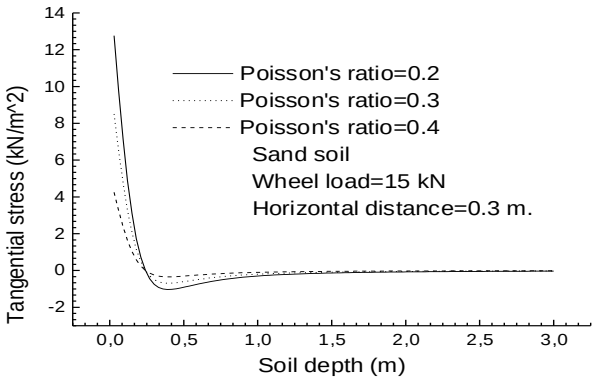

(a)

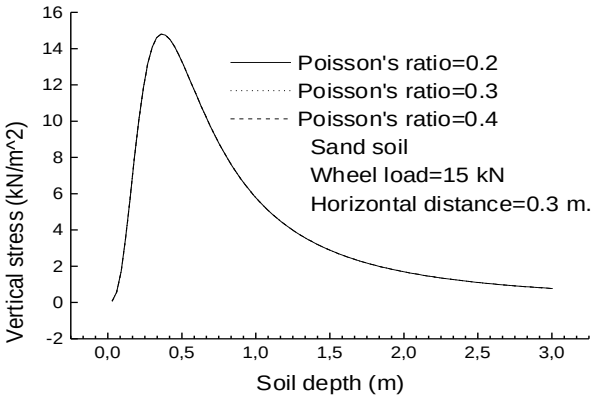

(b)

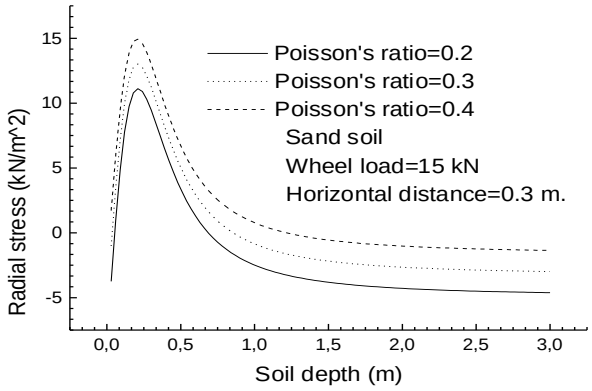

(c)

Fig. 11 Vertical, radial and tangential soil stresses distribution along the soil depth with the variation of Possion's ratio.

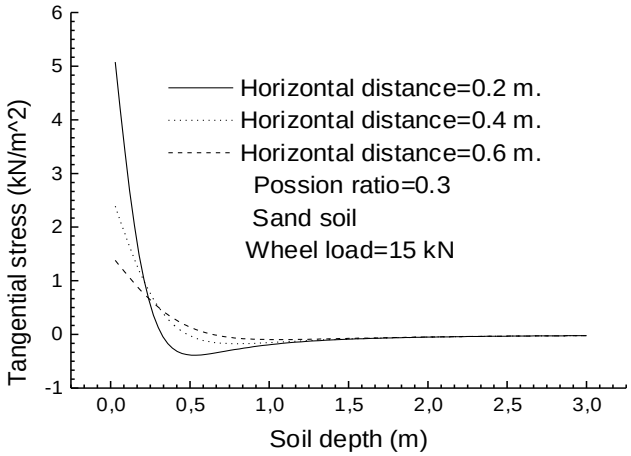

(a)

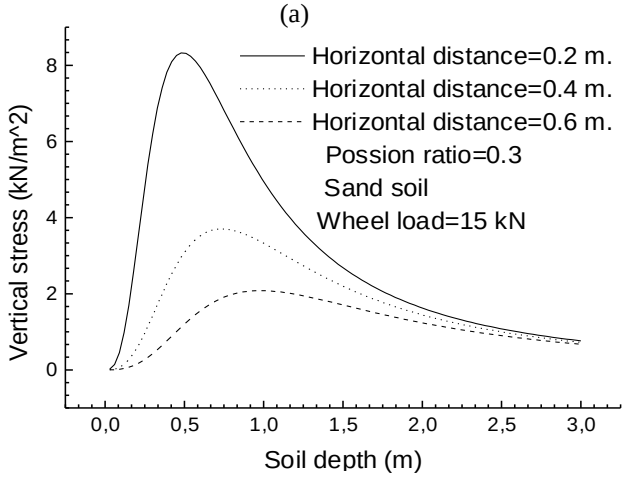

(b)

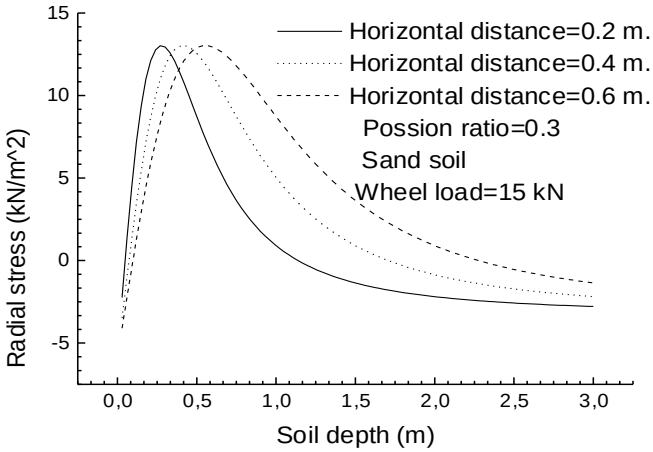

(c)

Fig. 12 Vertical, radial and tangential soil stresses distribution along the soil depth under the tyre

International Journal of Engineering Research & Technology (IJERT)
ISSN: 2278-0181
Vol. 10 Issue 02, February-2021

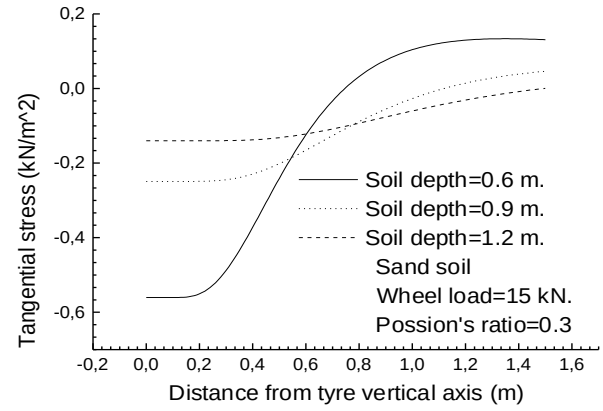

(a)

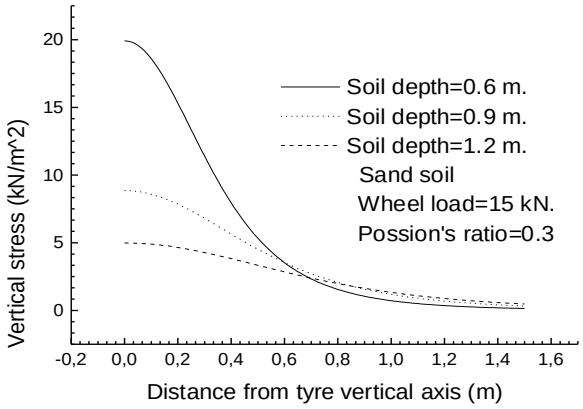

(b)

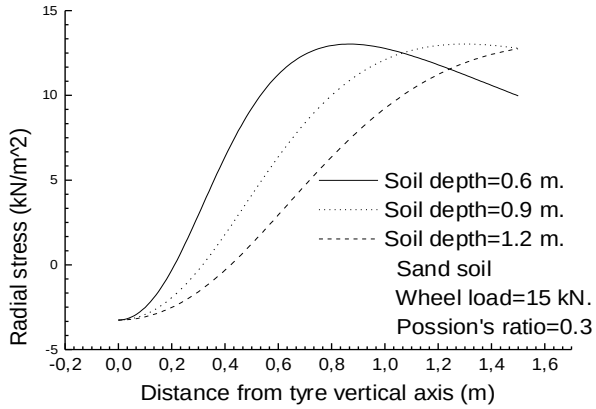

(c)

Fig. 13 Vertical, radial and tangential soil stresses distribution along the horizontal distance with the variation of soil depth.